

## Short Communication

# $(\alpha\text{-Fe}_2\text{O}_3)\text{-MCM-41-SO}_3\text{H}$ as a novel magnetic nanocatalyst for the synthesis of N-aryl-2-amino-1,6-naphthyridine derivatives

Shahnaz Rostamizadeh <sup>a,\*</sup>, Mohammad Azad <sup>a</sup>, Nasrin Shadjou <sup>a</sup>, Mohammad Hasanzadeh <sup>b</sup><sup>a</sup> Department of Chemistry, K. N. Toosi University of Technology, P.O. Box 15875-4416, Tehran, Iran<sup>b</sup> Drug Applied Research Center, Tabriz University of Medical Science, Tabriz, Iran

## ARTICLE INFO

## Article history:

Received 15 February 2012

Received in revised form 10 April 2012

Accepted 12 April 2012

Available online 21 April 2012

## Keywords:

Magnetic nanocatalyst

Heterogeneous catalyst

Sulfonic acid

N-aryl-2-amino-1,6-naphthyridines

## ABSTRACT

The new  $(\alpha\text{-Fe}_2\text{O}_3)\text{-MCM-41-SO}_3\text{H}$  catalyst was prepared directly through the reaction of chlorosulfonic acid with silica-coated nanoparticles  $(\alpha\text{-Fe}_2\text{O}_3)\text{-MCM-41}$  and used as a magnetically recyclable catalyst for an efficient one-pot synthesis of N-aryl-2-amino-1,6-naphthyridine derivatives. The catalyst with 10 wt% of loaded iron oxide nanoparticles could be recovered from the reaction mixture by an external magnet and reused without significant decrease in activity even after 5 runs. This new prepared catalyst exhibited better activities to other commercially available sulfonic acid catalysts.

© 2012 Elsevier B.V. All rights reserved.

## 1. Introduction

Acidic catalysts are widely used in a variety of organic transformations, such as aldol condensations, hydrolysis, acylations, and nucleophilic additions. However, use of soluble or liquid acids (homogeneous catalysts) has been inhibited in manufacturing synthesis because of difficulty in their waste neutralization, separations, reactor corrosion, and reusability [1].

The recovery and reusability of the catalyst are the two most important features for many catalytic processes. Hence, one efficient way to overcome the problem of homogeneous catalysts is the heterogenization of active catalytic molecules, creating a heterogeneous catalytic system. In contrast, the recovery of the most heterogeneous catalysts from the final reaction systems requires a filtration or centrifugation step and/or a tedious workup. For this purpose, by applying magnetic supports and an external magnet the catalysts can be easily recovered and subsequently reused in another cycle without significant decrease in their activity.

MCM-41 is an ordered mesoporous material which has only mildly acidic sites [2,3]. In order to promote their acidic character, sulfonic acid groups have been covalently bonded to these supports by various methods such as, oxidation of attached thiols [4], hydrolysis of sulfonic acid chlorides [5], sulfonation of supported phenyl groups [6], ring opening of perfluorosulfonic acid sultones [7,8], and immobilization of perfluorosulfonic acid triethoxysilanes [9]. It should be mentioned

that covalent anchoring of various molecules on silica surfaces is based on the presence of silanol groups [10].

Hence, for the first time the present work illustrates the immobilization of sulfonic acid groups on silica coated magnetic nanoparticles for its use as recyclable, solid acid catalyst for the synthesis of N-aryl-2-amino-1,6-naphthyridine derivatives.

Over the past few years, naphthyridine derivatives have received considerable attention because of their wide range of biological and pharmaceutical activities, such as antitumor, anti-inflammatory, and antifungal properties [11–13]. These compounds are very useful in the treatment of hypertension, myocardial infarction, hyperlipidemia, cardiac arrhythmia, and rheumatoid arthritis [14–16].

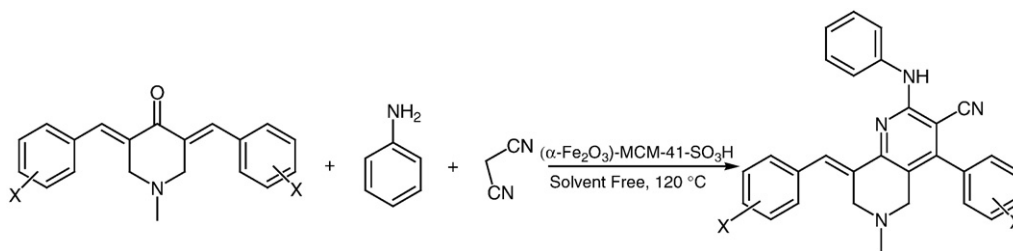
In view of these useful properties, and since we were interested in the synthesis of N-aryl-2-amino-1,6-naphthyridine derivatives, a literature survey revealed that there are only a few reports for the synthesis of these compounds. El-Subbagh et al. have reported the synthesis of 1,6-naphthyridine derivatives through the two component reaction of  $\alpha,\beta$ -unsaturated ketones and cyanoacetamide in butanol [12]. Recently, Shu-Jiang Tu et al. [17] reported the synthesis of N-aryl-2-amino-1,6-naphthyridine derivatives through three component reaction between  $\alpha,\beta$ -unsaturated ketones, aniline, and malononitrile using microwave irradiation in the presence of acetic acid as catalyst.

However, these methods are time-consuming and use a lot of toxic solvents and reagents. Thus, the development of a green, simple, efficient, and general method for the synthesis of these widely used organic compounds, from readily available reagents, remains one of the major challenges in organic synthesis.

Therefore in this work, magnetic nanoparticles which have been embedded in MCM-41 and subsequently functionalized with chlorosulfonic

\* Corresponding author. Fax: +98 21 22853650.

E-mail addresses: [rostamizadeh@kntu.ac.ir](mailto:rostamizadeh@kntu.ac.ir), [shrostamizadeh@yahoo.com](mailto:shrostamizadeh@yahoo.com) (S. Rostamizadeh).



**Scheme 1.**  $(\alpha\text{-Fe}_2\text{O}_3)\text{-MCM-41-SO}_3\text{H}$  as a magnetic catalyst for the synthesis of N-aryl-2-amino-1,6-naphthyridine derivatives.

acid [ $(\alpha\text{-Fe}_2\text{O}_3)\text{-MCM-41-SO}_3\text{H}$ ] have been used as new acidic catalyst for the one-pot synthesis of N-aryl-2-amino-1,6-naphthyridine derivatives under solvent free conditions (Scheme 1).

## 2. Experimental

Melting points were recorded on a Buchi B-540 apparatus. IR spectra were recorded on an ABB Bomem Model FTLA200-100 instrument.  $^1\text{H}$  and  $^{13}\text{C}$  NMR spectra were measured on a Bruker DRX-300 spectrometer, at 300 and 75 MHz, using TMS as an internal standard. Chemical shifts ( $\delta$ ) were reported relative to TMS, and coupling constants ( $J$ ) were reported in hertz (Hz). Mass spectra were recorded on a Shimadzu QP 1100 EX mass spectrometer with 70-eV ionization potential. X-ray powder diffraction (XRD) was carried out on a Philips X'Pert diffractometer with  $\text{CuK}\alpha$  radiation. The pore structure of the prepared catalyst was verified by the nitrogen sorption isotherm ([5.0.0.3] Belsorp, BEL Japan, Inc.). Transmission electron microscope (TEM) was recorded on a Philips CM-10 instrument on an accelerating voltage of 100 kV.

### 2.1. Catalyst preparation

A solution with molar composition of 3.2  $\text{FeCl}_3$ :1.6  $\text{FeCl}_2$ :1 CTABr:39  $\text{NH}_4\text{OH}$ :2300  $\text{H}_2\text{O}$  was used for preparation of naked  $\text{Fe}_3\text{O}_4$  nanoparticles at room temperature. Typically, 2 g of iron (III) chloride ( $\text{FeCl}_3 \cdot 6\text{H}_2\text{O}$ ) and 0.8 g of iron (II) chloride ( $\text{FeCl}_2 \cdot 4\text{H}_2\text{O}$ ) were dissolved in 10 mL of distilled water under  $\text{N}_2$  atmosphere. The resulting solution was added dropwise to a 100 mL solution of 1.0 M  $\text{NH}_4\text{OH}$  solution containing 0.4 g of cetyltrimethylammonium bromide (CTABr) to construct a colloidal suspension of iron oxide magnetic nanoparticles. The magnetic MCM-41 was prepared by adding 20 mL of the magnetic colloid to a 1 L solution with the molar composition of 292  $\text{NH}_4\text{OH}$ :1 CTABr:2773  $\text{H}_2\text{O}$  under vigorous mixing and sonication. Then sodium silicate (16 mL) was added, and the mixture was allowed to react at room temperature for 24 h under well-mixed conditions. The magnetic MCM-41 [ $(\text{Fe}_3\text{O}_4)\text{-MCM-41}$ ] was filtered and washed with alcoholic

ammonium nitrate. The surfactant template was then removed from the synthesized material by calcination at 450 °C for 4 h to give the [ $(\alpha\text{-Fe}_2\text{O}_3)\text{-MCM-41}$ ].

### 2.2. Preparation of $(\alpha\text{-Fe}_2\text{O}_3)\text{-MCM-41-SO}_3\text{H}$

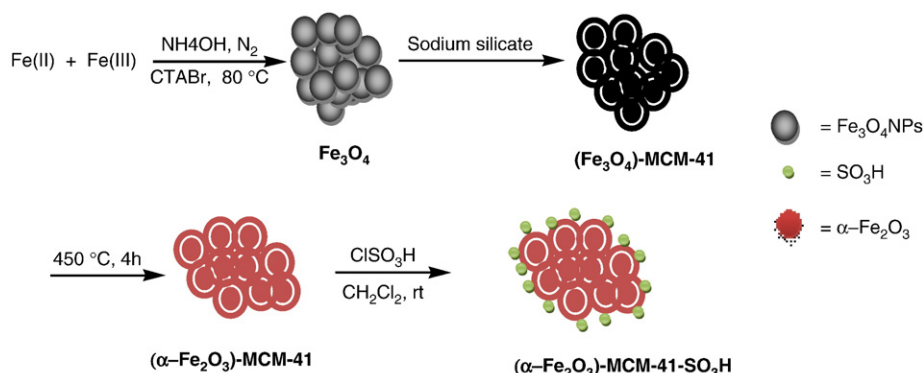
To  $(\alpha\text{-Fe}_2\text{O}_3)\text{-MCM-41}$  (1 g), chlorosulfonic acid (1 g, 9 mmol) in 5 mL dichloromethane was added dropwise at room temperature during 30 min. After completion of the addition, the mixture was mechanically stirred for other 30 min until HCl was removed from reaction vessel. The mixture was then filtered and washed with  $\text{CH}_2\text{Cl}_2$  to give  $(\alpha\text{-Fe}_2\text{O}_3)\text{-MCM-41-SO}_3\text{H}$  as brown powder. The amount of sulfonic acid groups of  $(\alpha\text{-Fe}_2\text{O}_3)\text{-MCM-41-SO}_3\text{H}$  which were determined by acid–base titration was found to be (0.56  $\text{SO}_3\text{H}$  per g).

### 2.3. General procedure for the synthesis of 3,5-dibenzylidenepiperidin-4-one [12]

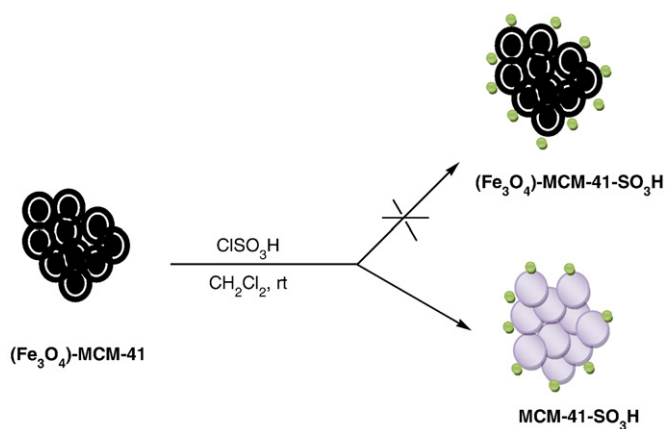
In a 50-mL reaction vial, a mixture of the 4-piperidone (10 mmol), the appropriate aldehyde (20 mmol), 10% NaOH (1 mL) and 95% EtOH (30 mL) was stirred at room temperature for 0.5–2 h. The separated solid was collected by filtration and for further purification was recrystallized from ethanol.

### 2.4. General procedure for the synthesis of N-aryl-2-amino-1,6-naphthyridine derivatives

To the mixture of 3,5-dibenzylidenepiperidin-4-one (0.33 mmol), aniline (0.33 mmol), and malononitrile (0.33 mmol) was added  $(\alpha\text{-Fe}_2\text{O}_3)\text{-MCM-41-SO}_3\text{H}$  (40 mg); it was then stirred at 120 °C for an appropriate period of time (Table 4). After completion of the reaction (monitored by thin-layer chromatography, TLC; petroleum ether and EtOAc, 1:1), the ethanol was added to the reaction mixture and the catalyst was collected with an external magnet. Then, the mixture was filtered and the



**Scheme 2.** Preparation of  $(\alpha\text{-Fe}_2\text{O}_3)\text{-MCM-41-SO}_3\text{H}$ .



**Scheme 3.** Reaction of  $(\text{Fe}_3\text{O}_4)\text{-MCM-41-SO}_3\text{H}$  with chlorosulfonic acid.

product was further purified by recrystallization from EtOH/H<sub>2</sub>O (1:1) to give the pure product.

### 3. Results and discussion

At first the  $(\alpha\text{-Fe}_2\text{O}_3)\text{-MCM-41}$  with 10 wt% of loaded iron oxide nanoparticles was prepared according to the reported method in the literature with some modifications [18] (Scheme 2).

In order to prepare  $[(\text{Fe}_3\text{O}_4)\text{-MCM-41-SO}_3\text{H}]$ , 1 g of uncalcined catalyst  $[(\text{Fe}_3\text{O}_4)\text{-MCM-41}]$  was reacted with 1 g chlorosulfonic acid in 5 mL dichloromethan. However because of the low stability of  $\text{Fe}_3\text{O}_4$  nanoparticles in the presence of chlorosulfonic acid, the desired catalyst  $[(\text{Fe}_3\text{O}_4)\text{-MCM-41-SO}_3\text{H}]$  was not formed and nonmagnetic catalyst  $(\text{MCM-41-SO}_3\text{H})$  was obtained (Scheme 3). Therefore,  $[(\text{Fe}_3\text{O}_4)\text{-MCM-41}]$  was calcined at 450 °C and converted to its stable form  $[(\alpha\text{-Fe}_2\text{O}_3)\text{-MCM-41}]$  [19,20]. It was then modified with chlorosulfonic acid to give the desired catalyst (Scheme 2).

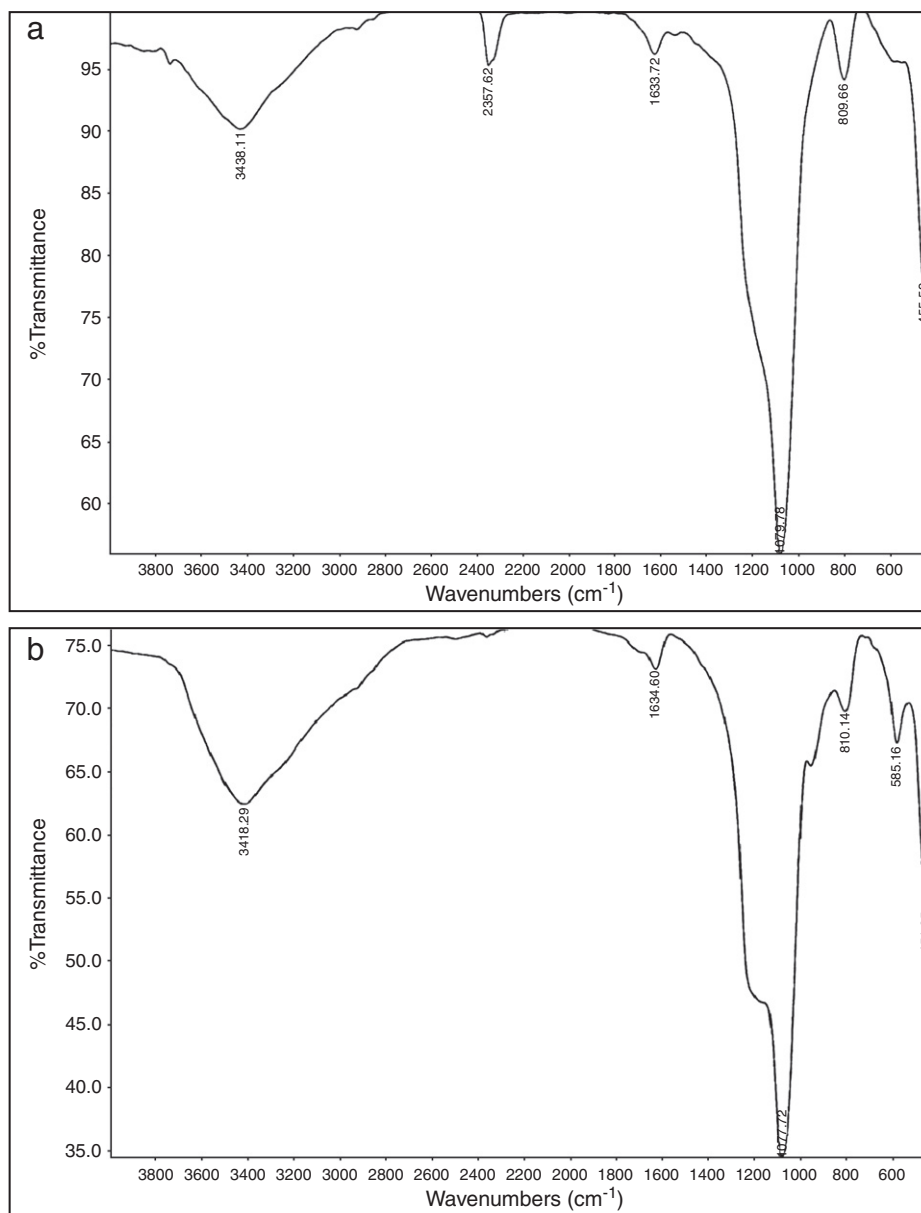


**Fig. 1.** The IR spectra of (a)  $(\alpha\text{-Fe}_2\text{O}_3)\text{-MCM-41}$ ; (b)  $(\alpha\text{-Fe}_2\text{O}_3)\text{-MCM-41-SO}_3\text{H}$ .

The prepared catalyst  $[(\alpha\text{-Fe}_2\text{O}_3)\text{-MCM-41-SO}_3\text{H}]$  was characterized with IR, XRD, SEM, TEM, nitrogen physisorption measurements, and acid–base titration. In FT-IR spectra the band in the region of  $400\text{--}650\text{ cm}^{-1}$  is attributed to the stretching vibrations of the (Fe–O) bond in  $\alpha\text{-Fe}_2\text{O}_3$ , and the band at about  $1100\text{ cm}^{-1}$  belongs to (Si–O) stretching vibrations (Fig. 1a and b). The peaks placed in  $1047$  and  $1220\text{ cm}^{-1}$  are related to the stretching of the SO bonds. A peak appeared at about  $3400\text{ cm}^{-1}$  due to the stretching of OH groups in the  $\text{SO}_3\text{H}$  (Fig. 1b).

The XRD patterns of the synthesized catalyst are presented in Fig. 2. The XRD analysis was performed from  $1.0^\circ (2\theta)$  to  $10.0^\circ (2\theta)$ , and  $10.0^\circ (2\theta)$  to  $80.0^\circ (2\theta)$ . The sample of  $(\alpha\text{-Fe}_2\text{O}_3)\text{-MCM-41-SO}_3\text{H}$  showed relatively well-defined XRD patterns, with one major peak along with

two small peaks identical to those of MCM-41 materials (Fig. 2a). In addition, XRD pattern in the region of  $10.0^\circ (2\theta)$  to  $80.0^\circ (2\theta)$  confirmed that change of sample's color from black to brick-red after calcination of the catalyst is due to the oxidation of embedded  $\text{Fe}_3\text{O}_4$  to  $\alpha\text{-Fe}_2\text{O}_3$  nanoparticles (Fig. 2b).

Also the SEM (Fig. 3a and b) and the TEM (Fig. 3c and d) showed that the embedded nanoparticles were present as uniform particles with spherical morphology.

The  $\text{N}_2$  adsorption isotherms after grafting of  $\text{SO}_3\text{H}$  group were recorded and shown in Fig. 4. The specific surface area and total pore volume obtained by the  $\text{N}_2$  adsorption isotherms and calculated by the Brunauer–Emmett–Teller (BET) method [21] were  $1024\text{ m}^2\text{ g}^{-1}$  and  $1.25\text{ cm}^3\text{ g}^{-1}$ , respectively. The pore diameter of the  $(\alpha\text{-Fe}_2\text{O}_3)\text{-}$

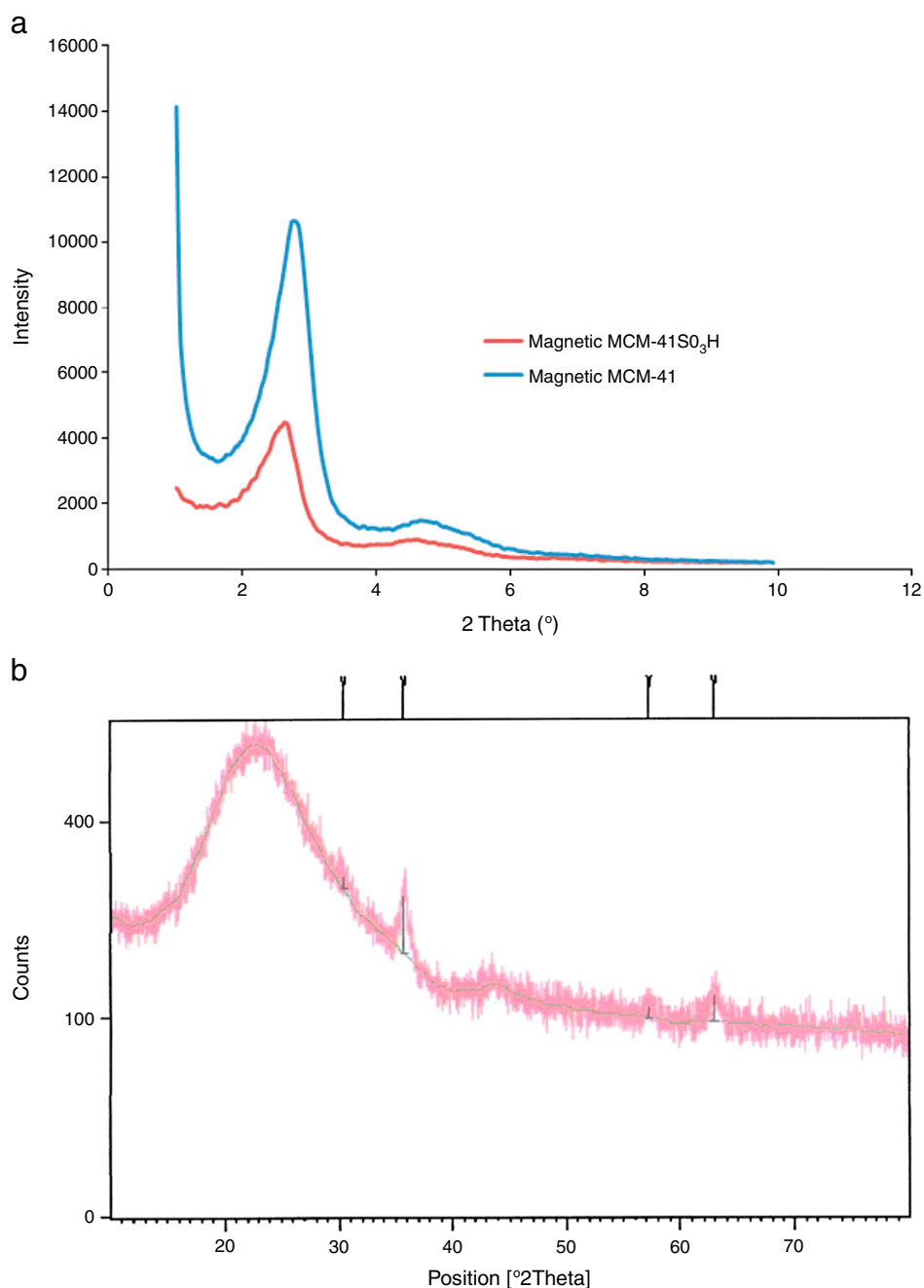


Fig. 2. (a) The XRD patterns of the  $(\alpha\text{-Fe}_2\text{O}_3)\text{-MCM-41}$  and  $(\alpha\text{-Fe}_2\text{O}_3)\text{-MCM-41-SO}_3\text{H}$  in the region of  $1.0^\circ (2\theta)$  to  $10.0^\circ (2\theta)$ . (b) The XRD patterns of  $(\alpha\text{-Fe}_2\text{O}_3)\text{-MCM-41-SO}_3\text{H}$  in the region of  $10.0^\circ (2\theta)$  to  $80.0^\circ (2\theta)$ .

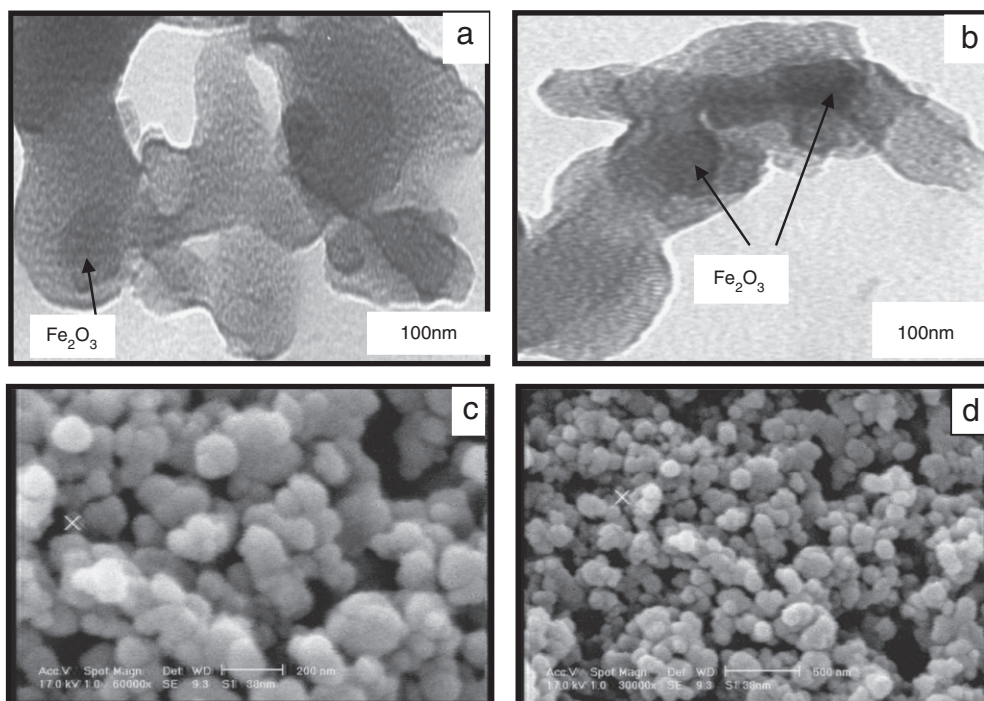


Fig. 3. The TEM (a, b) and SEM (c, d) images of  $(\alpha\text{-Fe}_2\text{O}_3)\text{-MCM-41-SO}_3\text{H}$ .

MCM-41-SO<sub>3</sub>H was 4.89 nm derived from the adsorption and desorption branches by the Broekhoff and deBoer model [22]. Also, detailed textural properties of  $(\alpha\text{-Fe}_2\text{O}_3)\text{-MCM-41}$  and  $(\alpha\text{-Fe}_2\text{O}_3)\text{-MCM-41-SO}_3\text{H}$  are summarized in Table 1, in which the surface area and pore volume of functionalized magnetic MCM-41 were lower than those of corresponding mesoporous silica due to the grafting of -SO<sub>3</sub>H groups.

The FT-IR analysis of the recovered catalyst after the reaction was recorded in which no sign of degradation of the anchored sulfonic acid

groups as well as leaching of embedded nanoparticles was observed (Fig. 5).

For optimization of the reaction conditions, 3,5-bis(4-chlorobenzylidene)-1-methylpiperidin-4-one (0.33 mmol), aniline (0.33 mmol), and malononitrile (0.33 mmol) were used as model reactants under solvent-free conditions (Scheme 4). At first, in order to show the unique catalytic behavior of  $(\alpha\text{-Fe}_2\text{O}_3)\text{-MCM-41-SO}_3\text{H}$  and to compare its activity with other catalysts, this reaction was performed in

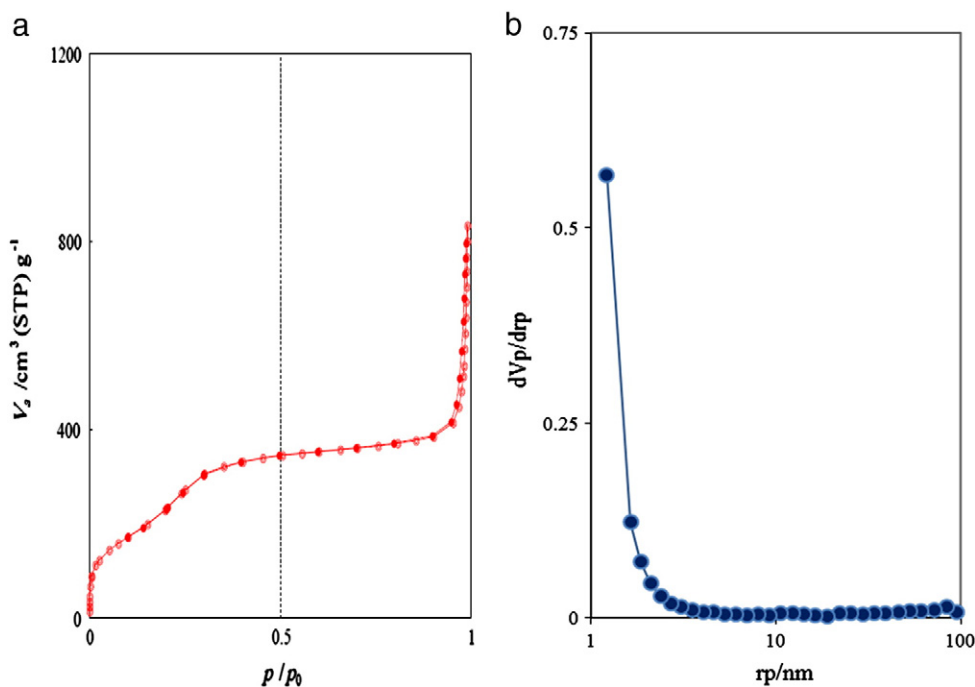


Fig. 4. (a) Nitrogen adsorption/desorption isotherm and (b) BJH of  $(\alpha\text{-Fe}_2\text{O}_3)\text{-MCM-41-SO}_3\text{H}$ .

**Table 1**

Surface area, average pore size, and pore volume of ( $\alpha$ -Fe<sub>2</sub>O<sub>3</sub>)-MCM-41 and ( $\alpha$ -Fe<sub>2</sub>O<sub>3</sub>)-MCM-41-SO<sub>3</sub>H.

Adsorbent	Surface area (m <sup>2</sup> g <sup>-1</sup> )	Average pore size (nm) <sup>a</sup>	Pore volume (cm <sup>3</sup> g <sup>-1</sup> ) <sup>b</sup>
( $\alpha$ -Fe <sub>2</sub> O <sub>3</sub> )-MCM-41	1213	5.26	1.59
( $\alpha$ -Fe <sub>2</sub> O <sub>3</sub> )-MCM-41-SO <sub>3</sub> H	1024	4.89	1.25

<sup>a</sup> Pore size is calculated by method described by Brunauer–Emmett–Teller.

<sup>b</sup> Pore volume determined from nitrogen physisorption isotherm.

the presence of catalytic amount of H<sub>3</sub>PW<sub>12</sub>O<sub>40</sub>, HClO<sub>4</sub>/SiO<sub>2</sub>, NaHSO<sub>4</sub>/SiO<sub>2</sub>, NaHSO<sub>4</sub>, MCM-41, ( $\alpha$ -Fe<sub>2</sub>O<sub>3</sub>)-MCM-41 and nanocrystalline metal oxides such as CuO and Fe<sub>3</sub>O<sub>4</sub> nanoparticles (Table 2). It was observed that only acidic catalysts were able to catalyze this reaction (Table 2, entry 2–5, 11). Also, at the first glance, according to reported method by Shu-Jiang Tu et al. [17], running the reaction in acetic acid at 110 °C, under microwave condition at 200 W, seemed appealing (Table 2, entry 8). Yet, such a procedure suffers from using an extra reagent (ammonium acetate) along with a toxic solvent (DMF) as well as employment of possibly harmful and rather expensive electromagnetic waves. [23]. Hence, it seems that the ( $\alpha$ -Fe<sub>2</sub>O<sub>3</sub>)-MCM-41-SO<sub>3</sub>H is the most effective catalyst for this purpose, leading to the synthesis of N-aryl-2-amino-1,6-naphthyridine derivatives in higher yields and shorter reaction times. The efficiency of this catalyst is due to the synergistic effect of Brønsted acidity of -SO<sub>3</sub>H and Lewis acidity of the Fe<sup>3+</sup> groups.

**Table 2**

Comparing the efficiency of different catalysts in the synthesis of **6d**.

Entry	Catalyst <sup>a</sup>	Time (min)	Yield (%)
1	No catalyst	180	trace
2	H <sub>3</sub> PW <sub>12</sub> O <sub>40</sub>	180	45
3	HClO <sub>4</sub> /SiO <sub>2</sub>	180	50
4	NaHSO <sub>4</sub> /SiO <sub>2</sub>	180	47
5	NaHSO <sub>4</sub>	240	35
6	Nano CuO	300	Trace
7	Fe <sub>3</sub> O <sub>4</sub> NPs	360	Trace
8	Acetic acid, MW, 110 °C, 200 W	5	96 [17]
9	MCM-41	180	Trace
10	( $\alpha$ -Fe <sub>2</sub> O <sub>3</sub> )-MCM-41	180	Trace
11	( $\alpha$ -Fe <sub>2</sub> O <sub>3</sub> )-MCM-41-SO <sub>3</sub> H	130	95

<sup>a</sup> Catalytic amount of all compared catalysts is 40 mg per 0.33 mmol of reactants.

**Table 3**

Solvent screening for the synthesis of **6d**.

Entry	Solvent	Time (min)	Yield (%)
1	DMF	135	70
2	Ethylenglycol	145	75
3	Dioxane	160	68
4	CH <sub>3</sub> CN	180	20
5	CH <sub>3</sub> OH	180	30
6	C <sub>2</sub> H <sub>5</sub> OH	180	30
7	H <sub>2</sub> O	180	No reaction
8	Solvent-free condition	130	95

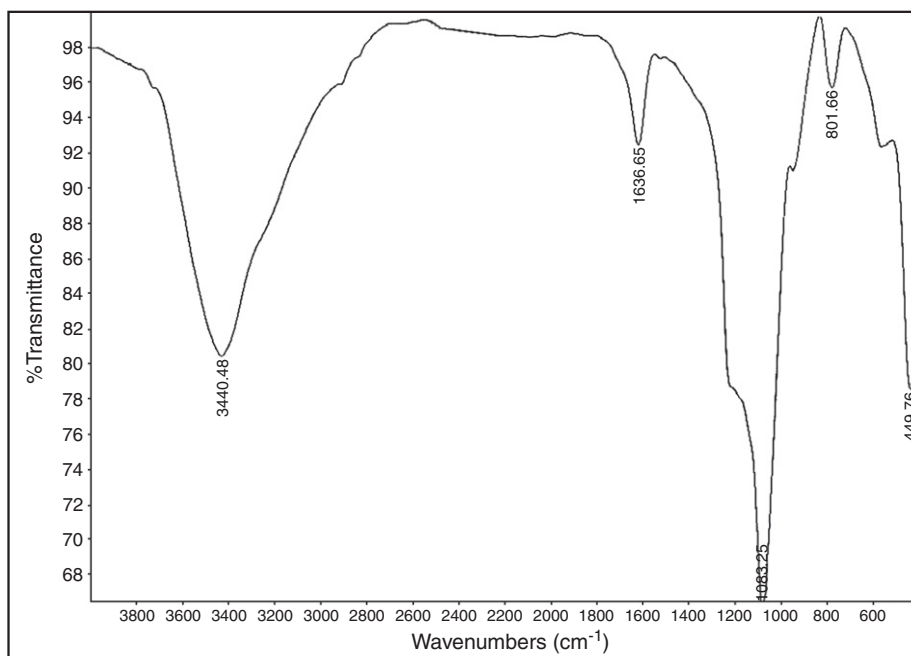
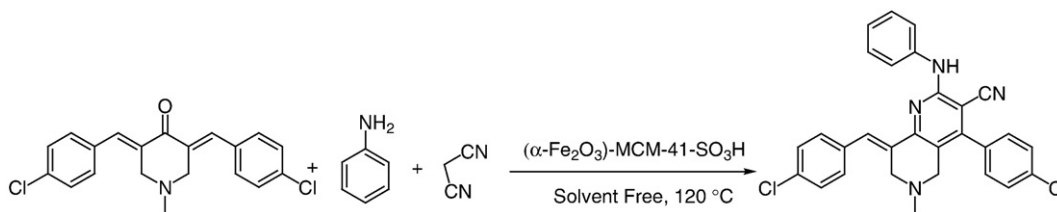
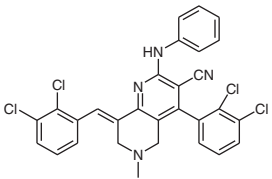
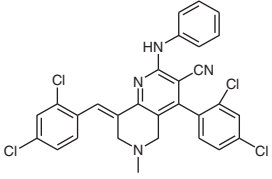
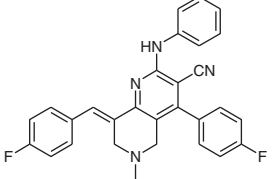
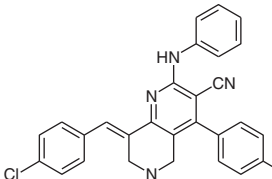
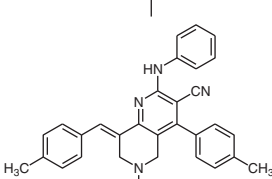
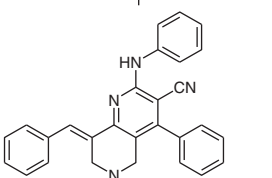
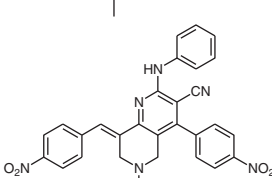
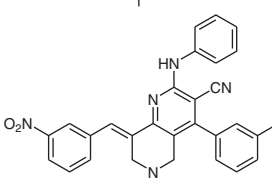
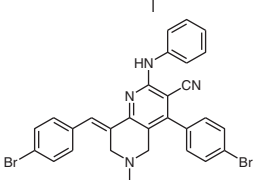


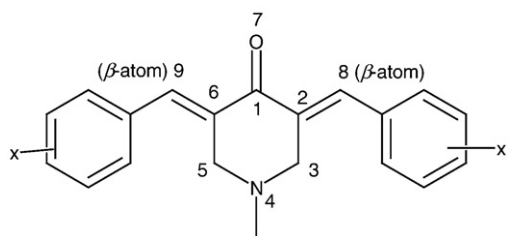
Fig. 5. The IR spectra of the recycled ( $\alpha$ -Fe<sub>2</sub>O<sub>3</sub>)-MCM-41-SO<sub>3</sub>H.



Scheme 4. Model reaction for the optimization.

**Table 4**  
The reaction time (min) and the yield (%) of N-aryl-2-amino-1,6-naphthyridine product.

Entry	Product	Time (min)	Yield (%)	M.P (°C) Found	M.P (°C) Reported
1	<b>6a</b> 	160	98	221–223	–
2	<b>6b</b> 	155	96	239–240	–
3	<b>6c</b> 	120	93	244–245	244–246 [17]
4	<b>6d</b> 	130	95	254–255	253–255 [17]
5	<b>6e</b> 	185	84	233–235	233–235 [17]
6	<b>6f</b> 	150	86	229–231	229–231 [17]
7	<b>6g</b> 	120	95	243–245	243–245 [17]
8	<b>6h</b> 	110	92	243–245	244–247 [17]
9	<b>6i</b> 	165	92	268–269	268–270 [17]



**Scheme 5.** The structure of 3,5-dibenzylidenepiperidin-4-one derivatives.

A comparison of the performance of the  $(\alpha\text{-Fe}_2\text{O}_3)\text{-MCM-41-SO}_3\text{H}$  in various solvents is shown in Table 3. Among the solvents tested (DMF, ethylenglycol, dioxane, acetonitrile, methanol, ethanol, water) and solvent-free conditions the latter gave the highest yields with shorter reaction times. This means that the higher concentration of reactants in the absence of solvents usually leads to more favorable kinetics than in solution [24]. Hence the solvent free condition has been selected as optimized condition.

After optimization of the reaction condition, a variety of aromatic aldehydes, possessing both electron-donating and electron-withdrawing groups, was employed for N-aryl-2-amino-1,6-naphthyridine formation, and the results indicated that for 3,5-dibenzylidenepiperidin-4-one bearing different functional groups, the reaction proceeded smoothly in all cases. It is worth mentioning that 3,5-dibenzylidenepiperidin-4-one with electron-withdrawing groups reacted rapidly whereas with those having electron-rich groups, longer reaction times were required. Electron-withdrawing groups on the phenyl rings (Table 4, entries 1–4, and 7–9) induce greater electronic positive charge on the corresponding  $\beta$ -atoms than electron donating moieties (Scheme 5).

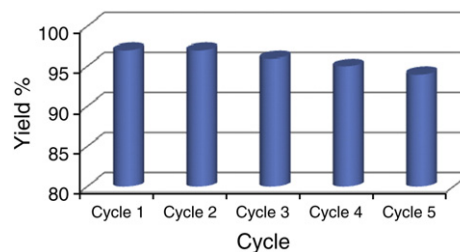
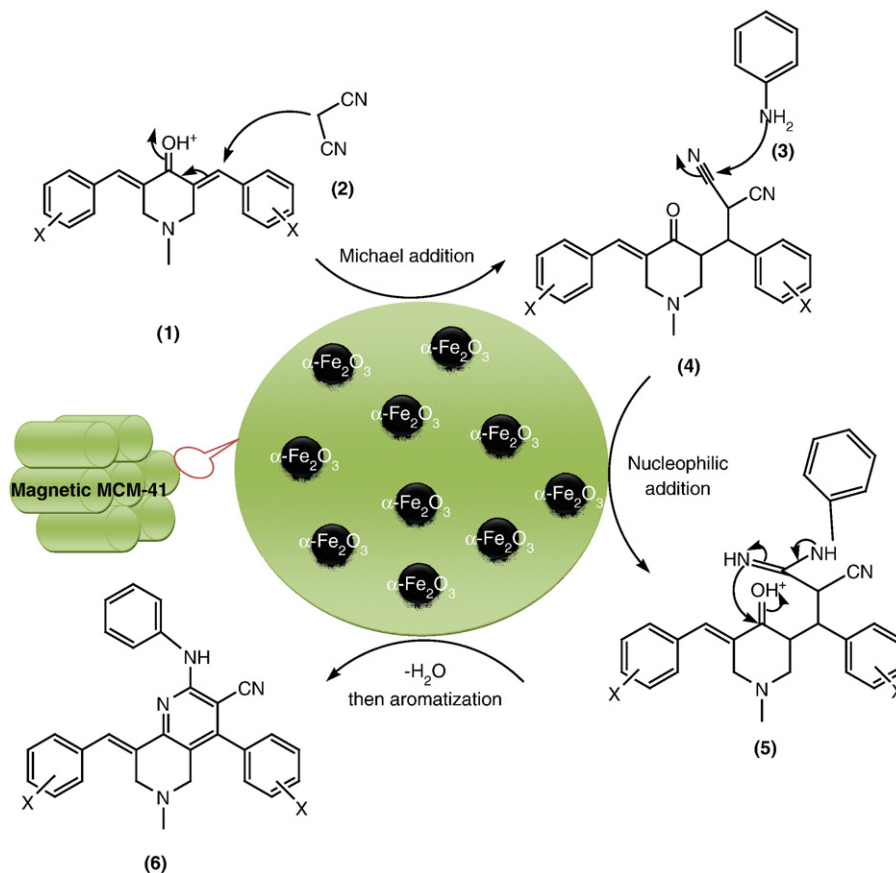


**Fig. 6.** Catalyst recovery at the end of the reaction.

The plausible mechanism is shown in Scheme 6. Because of two-dimensional pores of MCM-41, the reactants easily transfer toward the nanocatalyst channels, and they are accompanied by the inherent Brønsted acidity of  $\text{-SO}_3\text{H}$  and Lewis acidity of the  $\text{Fe}^{3+}$ , both of which are capable of bonding with the carbonyl oxygen of the 3,5-dibenzylidenepiperidin-4-one moiety. Afterwards, the Michael addition between activated 3,5-dibenzylidenepiperidin-4-one (1) and malononitrile (2) occurs, and then nucleophilic addition of aniline (3) to one of the cyano groups in the intermediate (4) results in the formation of the intermediate (5). Subsequently, through cyclization and aromatization, the product (6) is formed. In other words, ionic intermediates (4, 5) are generated inside the nanocatalyst because of the strong polarity of the  $\text{-SO}_3\text{H}$  and  $\text{Fe}^{3+}$  groups. Finally, by using this magnetic nanocatalyst, the reaction rates and yields under the reaction condition are enhanced (Scheme 6).

It is important to note that the magnetic property of this catalyst facilitates its efficient recovery from the reaction mixture during work-up procedure. In the presence of an external magnet, recoverable  $(\alpha\text{-Fe}_2\text{O}_3)\text{-MCM-41-SO}_3\text{H}$  moved onto the magnet steadily and the reaction



**Scheme 6.** A plausible mechanism for the synthesis of N-aryl-2-amino-1,6-naphthyridine in the presence of  $(\alpha\text{-Fe}_2\text{O}_3)\text{-MCM-41-SO}_3\text{H}$ .

mixture turned clear within 10 s. Thus, the catalyst effectively collected and the recovered catalyst was used in subsequent runs without observation of any significant decrease in activity even after 5 runs. (Fig. 6).

#### 4. Conclusion

In summary, the new ( $\alpha$ -Fe<sub>2</sub>O<sub>3</sub>)-MCM-41-SO<sub>3</sub>H catalyst was prepared directly through the reaction of chlorosulfonic acid with silica-coated nanoparticles ( $\alpha$ -Fe<sub>2</sub>O<sub>3</sub>)-MCM-41 and used as a magnetically recyclable catalyst for an efficient one-pot synthesis of N-aryl-2-amino-1,6-naphthyridine derivatives. The catalyst with 10 wt% of loaded iron oxide nanoparticles was separated with an external magnet, and was used in subsequent runs without observation of significant decrease in activity even after 5 runs. This new prepared catalyst exhibited better activities to other commercially available sulfonic acid catalysts.

#### Acknowledgements

We gratefully acknowledge the support of this work to K. N. Toosi University of Technology.

#### Appendix A. Supplementary data

Supplementary data to this article can be found online at [doi:10.1016/j.catcom.2012.04.013](https://doi.org/10.1016/j.catcom.2012.04.013).

#### References

- [1] A. Corma, H. Garcia, *Advanced Synthesis and Catalysis* 348 (2006) 1391–1412.
- [2] V. Polshettiwar, R. Luque, A. Fihri, H. Zhu, M. Bouhrara, J.M. Basset, *Chemical Reviews* 111 (2011) 3036–3075.
- [3] J.A. Melero, R. Grieken, G. Morales, *Chemical Reviews* 106 (2006) 3790–3812.
- [4] W.M. Van Rhijn, D.E. De Vos, B.F. Sels, W.D. Bossaert, P.A. Jacobs, *Chemical Communications* (1998) 317–318.
- [5] J.A. Melero, G.D. Stucky, R. Grieken, G. Morales, *Journal of Materials Chemistry* 12 (2002) 1664–1670.
- [6] C.W. Jones, K. Tsuji, M.E. Davis, *Microporous and Mesoporous Materials* 33 (1999) 223–240.
- [7] M. Alvaro, A. Corma, D. Das, V. Fornes, H. Garcia, *Chemical Communications* 8 (2004) 956–957.
- [8] M. Alvaro, A. Corma, D. Das, V. Fornes, H. Garcia, *Journal of Catalysis* 231 (2005) 48–55.
- [9] M.A. Harmer, Q. Sun, M.J. Michalczyk, Z.Y. Yang, *Chemical Communications* 18 (1997) 1803–1804.
- [10] A.P. Wight, M.E. Davis, *Chemical Reviews* 102 (2002) 3589–3614.
- [11] (a) M. Dukat, W. Fiedler, D. Dumas, I. Damaj, B. Martin, J.A. Rosecrans, J.R. James, R.A. Glennon, *European Journal of Medicinal Chemistry* 31 (1996) 875–888; (b) F.M. Romero, R. Ziessel, *Tetrahedron Letters* 36 (1995) 6471–6474; (c) M.U. Heller, S. Schubert, *The Journal of Organic Chemistry* 67 (2002) 8269–8272; (d) C. Kaes, A. Katz, M.W. Hosseini, *Chemical Reviews* 10 (2000) 3553–3590; (e) M. Iyoda, H. Otsuka, K. Sato, N. Nisato, M. Oda, *Bulletin. Chemical Society of Japan* 63 (1990) 80–87.
- [12] H.I. El-Subbagh, S.M. Abu-Zaid, M.A. Mahran, F.A. Badria, A.M. Al-Obaid, *Journal of Medicinal Chemistry* 43 (2000) 2915–2921.
- [13] A. Gangjee, Y. Zeng, J.J. McGuire, R.L. Kisliuk, *Journal of Medicinal Chemistry* 45 (2002) 5173–5181.
- [14] H.S. El-Kashef, A.A. Geies, A.M. Kamal El-Dean, A.A. Abdel-Hafez, *Journal of Chemical Technology and Biotechnology* 57 (1993) 15–19.
- [15] F. Haglid, *Ark Kemi* 26 (1967) 489–495.
- [16] J.S. Skotnicki, *Chem. Abstr.* 113 (1990) 78372 (U.S. Patent 4902685).
- [17] Z.-G. Han, C.-B. Miao, F. Shi, N. Ma, G. Zhang, S.-J. Tu, *Journal of Combinatorial Chemistry* 12 (2010) 16–19.
- [18] X. Chen, K.F. Lam, Q. Zhang, B. Pan, M. Arruebo, K.L. Yeung, *The Journal of Physical Chemistry. C* 113 (2009) 9804–9813.
- [19] Y. Li, H. Liao, Y. Qian, *Materials Research Bulletin* 33 (1998) 841–844.
- [20] F. Jiao, A. Harrison, J.-C. Jumas, A.V. Chadwick, W. Kockelmann, P.G. Bruce, *Journal of the American Chemical Society* 128 (2006) 5468–5474.
- [21] H. Takahashi, B. Li, T. Sasaki, C. Miyazaki, T. Kajino, S. Inagaki, *Microporous and Mesoporous Materials* 44–45 (2001) 755–762.
- [22] E.P. Barrett, L.G. Joyner, P.H. Halenda, *Journal of the American Chemical Society* 73 (1951) 373–385.
- [23] D. Rui, C. Daojun, Y. Yongjian, *Environmental Toxicology and Pharmacology* 31 (2011) 357–363.
- [24] K. Tanaka, *Solvent-free Organic Synthesis*, Wiley-VCH, Weinheim, 2003.